Sensorless Direct Torque Control for PM-Assisted Synchronous Motors With Injection High-Frequency Signal Into Stator Flux Reference Frame

Sensorless Direct Torque Control for PM-Assisted Synchronous Motors With Injection High-Frequency Signal Into Stator Flux Reference Frame

Paolo Guglielmi, Arzhang Yousefi-Talouki, Gianluca Iabichino, and Gianmario Pellegrino
Politecnico di Torino- Energy department
Corso Duca degli Abruzzi 24, Torino, Italy
paolo.guglielmi@polito.it

***Abstract*—A new sensorless direct torque control method for PM-Assisted synchronous motor drives is proposed in this paper. The stator flux linkage amplitude and electromagnetic torque are the two controlled variables which are regulated in stator flux frame. Unlike the two most conventional sensorless methods at low speeds, high frequency (HF) rotating carrier voltage injection into stationary reference frame and HF pulsating carrier voltage injection into estimated rotor reference frame, in this presented method, a HF flux signal is superimposed into the amplitude of the flux reference, i.e., to the stator flux reference, and then rotor position is estimated by demodulating the flux responses coming from flux observer. The advantage of the proposed method is that the HF signal is closed loop controlled thanks to the high bandwidth of the flux loop and that low pass filter (LPF) in torque and flux feedback loop is not required. Experimental results validate the feasibility of the proposed sensorless control technique and prove that the rotor position can be estimated accurately in both steady states and dynamics.**

Keywords—Direct torque control; flux observer; High-frequency signal injection; PM-Assisted motors; sensorless.

I. INTRODUCTION

Due to several advantages such as high efficiency, power density, and torque density, permanent magnet synchronous motors (PMSMs) have been penetrated in the market in recent decades [1-2]. Conventionally, direct torque control (DTC) and field oriented control (FOC) techniques are the well-known control schemes that are used for PSMS drives [3-4]. In the past decades, direct torque control (DTC) method has attracted extensive attentions due to its fast dynamic characteristic and robust implementation.

In general, ac motor drives need the knowledge of the rotor position coming from shaft mounted encoders which may increase the system cost, and reduce its reliability. Hence, sensorless control techniques can be good candidates to tackle these problems. Back-electromotive force (EMF) based and HF signal injection and magnetic saliency tracking based techniques are the two main categories for rotor position estimation in encoder-less control schemes. The back-EMF based sensorless control strategies are secured at medium and high speed levels, while at low speed and standstill, HF signal injection based methods are adopted [5-7].

In saliency based sensorless techniques, a HF signal is superimposed into the fundamental reference signal and then rotor position is retrieved by demodulating of corresponding HF signals. Conventionally, these techniques are divided into pulsating signal injection [8], and rotating signal injection [9]. In pulsating signal injection, a HF signal, usually voltage, is injected to the estimated rotor *d*-axis and the HF component of the current on q-axis is demodulated and eventually rotor position is extracted using a PLL tracking loop. In rotating high frequency signal injection techniques, a balanced three phase HF voltage is superimposed to the fundamental components stationary (α, β) coordinates. Then, by using the synchronous reference frame filter (SRFF), position of the rotor will be extracted. Conventionally, in all sensorless DTC methods presented in the literature hitherto, HF signals are injected to the estimated rotor *d*-sxis (pulsating voltage), or to the stationary reference frames (rotating voltage). Since in these methods, HF signal is injected after flux and torque PI regulators, the bandwidth of these PI regulators should be sufficiently low to keep the fundamental components far from HF components. Therefore, the fast dynamic of DTC may be sacrificed during high frequency injection.

A new sensorless control strategy for sensorless DTC of PM-assisted synchronous motors is proposed in this work. Unlike the presented methods in the literature, a HF flux component is superimposed to the flux reference amplitude and rotor position is estimated by demodulating the flux responses in both *d* and *q* estimated axis. Hence, the HF injected signal is closed loop controlled thanks to the high bandwidth of flux loop. Using this presented method, no filter is required in the torque and flux inner loops and therefore, the high bandwidth of PI regulators can be preserved.

II. THEORETICAL CONCEPT

A. PM-Assisted Synchronous reluctance motor equations

The adopted vector reference frame for PM-assisted synchronous reluctance (SyR) motor is reported in Fig.1, where (α, β), (d, q) and (d_s, q_s) stand for stationary frame, rotor flux frame, and stator flux frame, respectively.

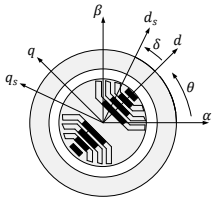

Fig. 1. Stationary, rotor flux, and stator flux reference frames.

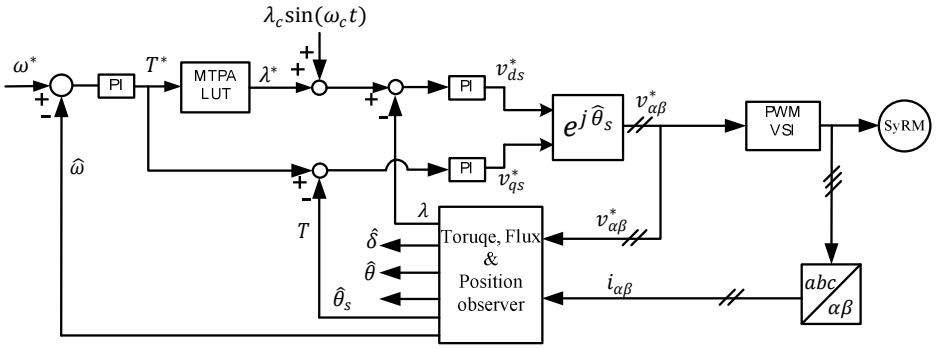

Fig. 2. Schematic diagram of sensorless DTC.

The dynamic equation of voltages and currents for PM-assisted SyRMs in *dq* rotor flux frame is expressed in (1), where R_s denotes for stator resistance, ω stands for rotor angular frequency, $\bar{v}_{dq}$ is stator voltage vector, $\bar{\imath}_{dq}$ denotes for stator current vector, and $\bar{\lambda}_{dq}$ is stator flux linkage vector. The magnetic model (2) is implemented in the form of two dimensional lookup tables. λ_m in (2) is the permanent magnet flux linkage.

$$\bar{v}_{dq} = R_s \bar{\imath}_{dq} + \frac{d\bar{\lambda}_{dq}}{dt} + j\omega\bar{\lambda}_{dq} \tag{1}$$

$$\begin{cases} \lambda_d = \lambda_d(i_d, i_q) = L_d(i_d, i_q)\,.\,i_d + \lambda_m \\ \lambda_q = \lambda_q(i_d, i_q) = L_q(i_d, i_q)\,.\,i_q \end{cases} \tag{2}$$

Equation (3) is obtained by rotating the voltage model (1) to the stator flux reference frame (d_s, q_s), where δ is the load angle and λ is the amplitude of the stator flux linkage vector [10-11].

$$\begin{cases} v_{ds} = R_s i_{ds} + \frac{d\lambda}{dt} \\ v_{qs} = R_s i_{qs} + \lambda \cdot (\omega + \frac{d\delta}{dt}) \end{cases} \tag{3}$$

B. Direct torque control

In DTC method, the electromagnetic torque and flux amplitude are the two controlled variables.

From (3) it is seen that the amplitude of stator flux is controlled using d_s-voltage channel. On the other hand, torque equation in stator flux frame can be written as (4) [10-11], where p denotes for pole pairs number. It is seen that if the amplitude of stator flux linkage (λ) is kept constant, electromagnetic torque is regulated by means of q_s-axis channel.

$$T = \frac{3}{2} \cdot p \cdot \lambda \cdot i_{qs} \tag{4}$$

The schematic diagram of sensorless DTC is shown in Fig.2. As seen, $\lambda_c \sin(\omega_c t)$ as a HF signal is injected to the flux reference which will be explained in the following.

C. Stator flux and electromagnetic torque observer

Fig.3 shows a combined voltage/current flux observer which is the combination of flux maps for low speed and back-EMF for high speeds. $\hat{\lambda}_{\alpha\beta}$ is the ultimate observed flux needed for the control and $\hat{\lambda}_{\alpha\beta,i}$ is the estimated flux coming from current to flux maps (current model). The transfer function of the adopted flux observer is as (5) where $g[\frac{rad}{s}]$ is the crossover speed between back-EMF integration and current to flux model. From (5) it is conclude that voltage model dominates if angular frequency is greater than g, while, when angular frequency is less than g, current model contributes. The outputs of the observer are amplitude of stator flux and phase angle as evidenced in Fig.3.

$$\hat{\lambda}_{\alpha\beta} = \frac{s}{s+g}\left(\frac{v_{\alpha\beta}^* - R_S\,.\,i_{\alpha\beta}}{s}\right) + \frac{g}{s+g}\hat{\lambda}_{\alpha\beta,i} \tag{5}$$

Using the observed flux, electromagnetic torque is estimated by used of equation (6).

$$\hat{T}_e = \frac{3}{2} \cdot p \cdot (\hat{\lambda}_\alpha \cdot i_\beta - \hat{\lambda}_\beta \cdot i_\alpha) \tag{6}$$

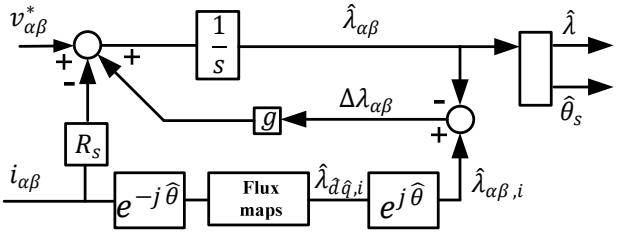

Fig. 3. Stator flux observer.

III. PROPOSED SENSORLESS DTC

Fig.4 illustrates the estimated frames and HF injection where, $(\hat{d}, \hat{q})$ is the estimated rotor frame and $(\hat{d}_s, \hat{q}_s)$ is the estimated stator reference frame. λ_c is the amplitude of the injected flux and ω_c is the angular frequency. As can be seen, a HF flux component is injected to the estimated $\hat{d}_s$-axis of flux frame.

When a HF signal is injected to the motor, the HF flux components in rotor *dq* frame is as (7), where subscript "*HF*"

denotes for HF signal and L_{dd} and L_{qq} are incremental inductances.

$$\begin{bmatrix}\lambda_{d,HF}\\ \lambda_{q,HF}\end{bmatrix}=\begin{bmatrix}L_{dd} & 0\\ 0 & L_{qq}\end{bmatrix}\begin{bmatrix}I_{d,HF}\\ I_{q,HF}\end{bmatrix} \quad (7)$$

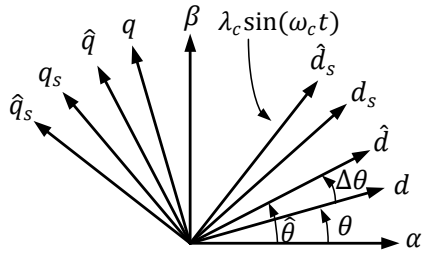

Fig. 4. Different reference frames used in sensorless control.

With rotating (7) to stationary $\alpha\beta$ frame, it is obtained that:

$$\lambda_{\alpha\beta,HF}=[L_{cm}]i_{\alpha\beta,HF}+A(-2\theta)[L_{dm}]i_{\alpha\beta,HF} \quad (8)$$

Where,

$$[L_{cm}]=\begin{bmatrix}L_{cm} & 0\\ 0 & L_{cm}\end{bmatrix} \quad (9)$$

$$[L_{dm}]=\begin{bmatrix}L_{dm} & 0\\ 0 & -L_{dm}\end{bmatrix} \quad (10)$$

$$A(2\theta)=\begin{bmatrix}\cos(2\theta) & \sin(2\theta)\\ -\sin(2\theta) & \cos(2\theta)\end{bmatrix} \quad (11)$$

$$L_{cm}=\frac{L_{dd}+L_{qq}}{2},\quad L_{dm}=\frac{L_{dd}-L_{qq}}{2} \quad (12)$$

If equation (8) is rotated to the estimated rotor $(\hat{d},\hat{q})$ axis, the observed flux based on voltage model is obtained as (13):

$$\hat{\lambda}_{\hat{d}\hat{q},HF}=A(\hat{\theta})[L_{cm}]A(-\hat{\theta})i_{dq,HF}+A(\hat{\theta})A(-2\theta)[L_{dm}]A(-\hat{\theta})i_{dq,HF} \quad (13)$$

On the other hand, with rotating (8) to the estimated rotor frame, current model based observed flux is obtained as (14):

$$\hat{\lambda}_{\hat{d}\hat{q},HF,i}=A(\hat{\theta})[L_{cm}]A(-\hat{\theta})i_{dq,HF}+A(\hat{\theta})A(-2\hat{\theta})[L_{dm}]A(-\hat{\theta})i_{dq,HF} \quad (14)$$

From (13) and (14) and using (9)-(11) it is deduced that:

$$\begin{bmatrix}\hat{\lambda}_{\hat{d},HF}\\ \hat{\lambda}_{\hat{q},HF}\end{bmatrix}=\begin{bmatrix}L_{cm} & 0\\ 0 & L_{cm}\end{bmatrix}\begin{bmatrix}I_{dHF}\\ I_{qHF}\end{bmatrix}+\begin{bmatrix}L_{dm}\cos(2\Delta\theta) & -L_{dm}\sin(2\Delta\theta)\\ -L_{dm}\sin(2\Delta\theta) & -L_{dm}\cos(2\Delta\theta)\end{bmatrix}\begin{bmatrix}I_{dHF}\\ I_{qHF}\end{bmatrix} \quad (15)$$

$$\begin{bmatrix}\hat{\lambda}_{\hat{d},HF,i}\\ \hat{\lambda}_{\hat{q},HF,i}\end{bmatrix}=\begin{bmatrix}L_{cm} & 0\\ 0 & L_{cm}\end{bmatrix}\begin{bmatrix}I_{dHF}\\ I_{qHF}\end{bmatrix}+\begin{bmatrix}L_{dm} & 0\\ 0 & -L_{dm}\end{bmatrix}\begin{bmatrix}I_{dHF}\\ I_{qHF}\end{bmatrix} \quad (16)$$

With subtracting (15) from (16), it is obtained that:

$$\begin{bmatrix}\Delta\hat{\lambda}_{\hat{d}HF}\\ \Delta\hat{\lambda}_{\hat{q}HF}\end{bmatrix}=\begin{bmatrix}\hat{\lambda}_{\hat{d},HF,i}-\hat{\lambda}_{\hat{d},HF}\\ \hat{\lambda}_{\hat{q},HF,i}-\hat{\lambda}_{\hat{q},HF}\end{bmatrix} \quad (17)$$

Therefore,

$$\begin{bmatrix}\Delta\hat{\lambda}_{\hat{d}HF}\\ \Delta\hat{\lambda}_{\hat{q}HF}\end{bmatrix}=L_{dm}\begin{bmatrix}1-\cos(2\Delta\theta) & \sin(2\Delta\theta)\\ \sin(2\Delta\theta) & -1+\cos(2\Delta\theta)\end{bmatrix}\begin{bmatrix}I_{dHF}\\ I_{qHF}\end{bmatrix} \quad (18)$$

If rotor position estimation error $(\Delta\theta)$ is considered as a small angle, (18) can be written as bellow:

$$\begin{bmatrix}\Delta\hat{\lambda}_{\hat{d}HF}\\ \Delta\hat{\lambda}_{\hat{q}HF}\end{bmatrix}=L_{dm}\begin{bmatrix}0 & \sin(2\Delta\theta)\\ \sin(2\Delta\theta) & 0\end{bmatrix}\begin{bmatrix}I_{dHF}\\ I_{qHF}\end{bmatrix} \quad (19)$$

With subtracting $\Delta\hat{\lambda}_{\hat{q}HF}$ from $\Delta\hat{\lambda}_{\hat{d}HF}$, equation (20) is obtained:

$$\Delta\hat{\lambda}_{\hat{d}HF}-\Delta\hat{\lambda}_{\hat{q}HF}=L_{dm}\sin(2\Delta\theta)\left(I_{qHF}-I_{dHF}\right) \quad (20)$$

The term $\left(I_{qHF}-I_{dHF}\right)$ in (20) can be considered as (21), where coefficient A is dependent to different motor working points.

$$I_{qHF}-I_{dHF}=A\sin(\omega_c t) \quad (21)$$

Therefore, equation (20) can be written as bellow:

$$\Delta\hat{\lambda}_{\hat{d}HF}-\Delta\hat{\lambda}_{\hat{q}HF}=k\sin(2\Delta\theta)\sin(\omega_c t) \quad (22)$$

Where, coefficient k is dependent to motor working points and consequently electromagnetic torque.

$$k=f(T)=L_{dm}\cdot A \quad (23)$$

From (22), it is seen that the term $\Delta\hat{\lambda}_{\hat{d}HF}-\Delta\hat{\lambda}_{\hat{q}HF}$ is proportional to position estimation error $(\Delta\theta)$. Hence, to retrieve the rotor position, this signal should be demodulated and forced to zero using a PI regulator.

Fig.5 reports how $\Delta\hat{\lambda}_{\hat{d}}-\Delta\hat{\lambda}_{\hat{q}}$ signal is obtained from flux observer. Considering Fig.5 and above-mentioned mathematics, it is evident from Fig.6 that the $\Delta\hat{\lambda}_{\hat{d}HF}-\Delta\hat{\lambda}_{\hat{q}HF}$ signal is obtained using a band pass filter. Then, this signal $(\Delta\hat{\lambda}_{\hat{d}HF}-\Delta\hat{\lambda}_{\hat{q}HF})$ is demodulated and low pass filtered to achieve the position error signal ε as shown in Fig.6 and equation (24).

$$\varepsilon=LPF\left[\left(\Delta\hat{\lambda}_{\hat{d}HF}-\Delta\hat{\lambda}_{\hat{q}HF}\right)\cdot\sin(\omega_c t)\right]=\frac{k}{2}\cdot\sin(2\Delta\theta) \quad (24)$$

Equation (25) can be approximated if $\Delta\theta$ is assumed as a small angle.

$$\varepsilon \cong k \cdot \Delta\theta \qquad (25)$$

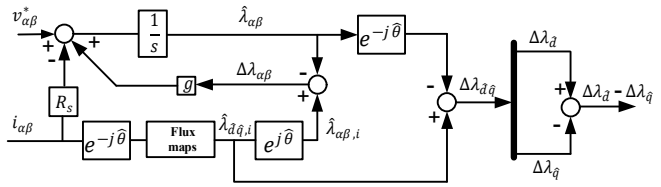

Fig. 5. Stator flux observer and corresponding flux signals for demodulation.

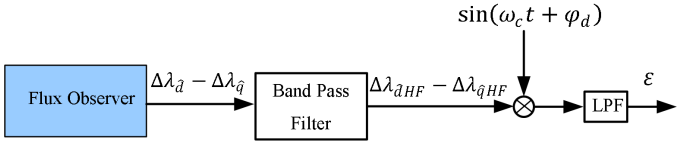

Fig. 6. Demodulation of $\Delta\lambda_{\hat{d}} - \Delta\lambda_q$ signal.

Eventually, a tracking loop is required to obtain the accurate rotor position as shown in Fig.7. As it is evident, the ε signal (25) is forced to zero using a PI regulator.

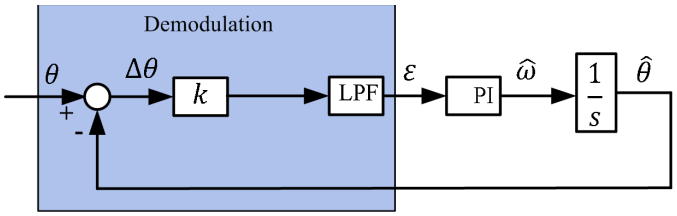

Fig. 7. Tracking loop for rotor position estimation.

IV. EXPERIMENTAL RESULTS

The proposed sensorless control is tested on an experimental drive test system and results are presented in this section. The experimental platform consists of a PM-assisted SyR motor, a load machine, a voltage source inverter (VSI), and a digital signal processor (DSP-MC56F827xx) controller. The specifications of the motor under test are tabulated in Table I. The results are presented in torque control and speed control modes.

TABLE I – PM-assistedSyR motor data

Nominal torque/Maximum torque [Nm]	1 / 3
Magnet flux [Vs]	.0064
Nominal speed/ Maximum speed [rpm]	3000/16000
Pole pairs	2
dc-link voltage [v]	280

A. Torque control test

Fig.8 reports the performance of the sensorless DTC in torque control mode while the speed is kept constant using a load drive. As seen, a ramp torque is imposed to the motor from 0.1 [Nm] to 1 [Nm] and vice versa. It is evident from this figure that $\Delta\theta$ angle is close to zero in both transients and steady state.

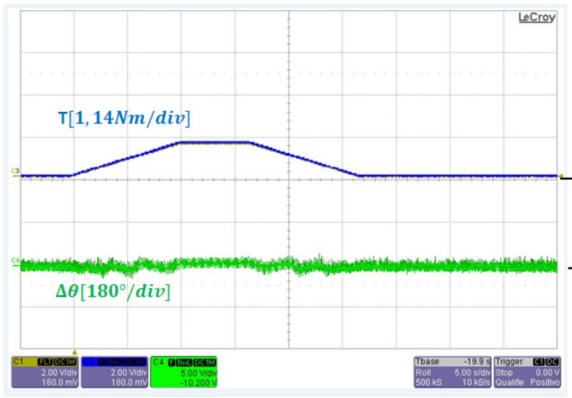

Fig. 8. Torque control test: from 0.1 [Nm] to 1 [Nm].

B. Speed control

The performance of the drive in speed control test is illustrated in Fig.9. As seen, the speed goes to 200 [rpm] from standstill and again decelerates to standstill. The position estimation error in both standstill and 200 [rpm] is near to zero.

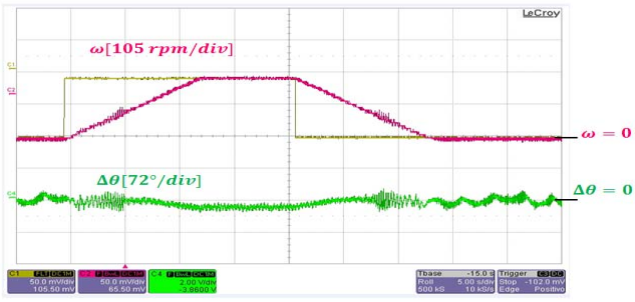

Fig. 9. Speed control test at no load.

V. CONCLUSION

A sensorless direct torque control method has been proposed for PM-assisted synchronous reluctance motor drives. A pulsating HF flux signal is injected to the estimated flux reference frame and HF flux responses in estimated rotor frame (both *d* and *q*-axis) are demodulated. The proposed sensorless technique was successfully validated by experiments and results have been presented.

REFERENCES

[1] A. M. El-Refaie and T. M. Jahns, "Comparison of synchronous PM machine types for wide constant-power speed range operation," *Fourtieth IAS Annual Meeting. Conference Record of the 2005 Industry Applications Conference, 2005.*, 2005, pp. 1015-1022 Vol. 2.

[2] G. Pellegrino, A. Vagati, B. Boazzo and P. Guglielmi, "Comparison of Induction and PM Synchronous Motor Drives for EV Application Including Design Examples," in IEEE Transactions on Industry Applications, vol. 48, no. 6, pp. 2322-2332, Nov.-Dec. 2012.

[3] Y. Yan, S. Wang, C. Xia, H. Wang and T. Shi, "Hybrid Control Set-Model Predictive Control for Field-Oriented Control of VSI-PMSM," in *IEEE Transactions on Energy Conversion*, vol. 31, no. 4, pp. 1622-1633, Dec. 2016.

[4] A. Yousefi-Talouki, S. A. Gholamian, M. Yousefi-Talouki, R. Ilka and A. Radan, "Harmonic elimination in switching table-based direct torque control of five-phase PMSM using matrix converter," *2012 IEEE*

Symposium on Humanities, Science and Engineering Research, Kuala Lumpur, 2012, pp. 777-782.

[5] G. Foo, S. Sayeef and M. F. Rahman, "Low-Speed and Standstill Operation of a Sensorless Direct Torque and Flux Controlled IPM Synchronous Motor Drive," in *IEEE Transactions on Energy Conversion*, vol. 25, no. 1, pp. 25-33, March 2010.

[6] T. Tuovinen and M. Hinkkanen, "Adaptive Full-Order Observer With High-Frequency Signal Injection for Synchronous Reluctance Motor Drives," in *IEEE Journal of Emerging and Selected Topics in Power Electronics*, vol. 2, no. 2, pp. 181-189, June 2014.

[7] P. Guglielmi, M. Pastorelli and A. Vagati, "Impact of cross-saturation in sensorless control of transverse-laminated synchronous reluctance motors," in *IEEE Transactions on Industrial Electronics*, vol. 53, no. 2, pp. 429-439, April 2006.

[8] Ji-Hoon Jang, Seung-Ki Sul, Jung-Ik Ha, K. Ide and M. Sawamura, "Sensorless drive of surface-mounted permanent-magnet motor by high-frequency signal injection based on magnetic saliency" in *IEEE Transactions on Industry Applications*, vol. 39, no. 4, pp. 1031-1039, July-Aug. 2003.

[9] P. L. Jansen and R. D. Lorenz, "Transducerless position and velocity estimation in induction and salient AC machines," in *IEEE Transactions on Industry Applications*, vol. 31, no. 2, pp. 240-247, Mar/Apr 1995.

[10] A. Yousefi-Talouki, P. Pescetto and G. Pellegrino, "Sensorless Direct Flux Vector Control of Synchronous Reluctance Motors Including Standstill, MTPA, and Flux Weakening," in *IEEE Transactions on Industry Applications*, vol. 53, no. 4, pp. 3598-3608, July-Aug. 2017.

[11] A. Yousefi-Talouki; P. Pescetto; G. Pellegrino; I. Boldea, "Combined Active Flux and High Frequency Injection Methods for Sensorless Direct Flux Vector Control of Synchronous Reluctance Machines," in IEEE Transactions on Power Electronics , vol.PP, no.99, pp.1-1.